



# LUND UNIVERSITY

## Data-flow Coupling and Data-Acquisition Triggers for the PreSPEC-AGATA Campaign at GSI

Ralet, D.; Pietri, S.; Aubert, Y.; Bellato, M.; Bortolato, D.; Brambilla, S.; Camera, F.; Dosme, N.; Gadea, A.; Gerl, J.; Golubev, Pavel; Grave, X.; Johansson, H. T.; Karkour, N.; Korichi, A.; Kurz, N.; Lafay, X.; Legay, E.; Linget, D.; Pietralla, N.; Rudolph, Dirk; Schaffner, H.; Stezowski, O.; Travers, B.; Wieland, O.

*Published in:*

Nuclear Instruments & Methods in Physics Research. Section A: Accelerators, Spectrometers, Detectors, and Associated Equipment

*DOI:*

[10.1016/j.nima.2015.03.025](https://doi.org/10.1016/j.nima.2015.03.025)

2015

[Link to publication](#)

*Citation for published version (APA):*

Ralet, D., Pietri, S., Aubert, Y., Bellato, M., Bortolato, D., Brambilla, S., Camera, F., Dosme, N., Gadea, A., Gerl, J., Golubev, P., Grave, X., Johansson, H. T., Karkour, N., Korichi, A., Kurz, N., Lafay, X., Legay, E., Linget, D., ... Wieland, O. (2015). Data-flow Coupling and Data-Acquisition Triggers for the PreSPEC-AGATA Campaign at GSI. *Nuclear Instruments & Methods in Physics Research. Section A: Accelerators, Spectrometers, Detectors, and Associated Equipment*, 786, 32-39. <https://doi.org/10.1016/j.nima.2015.03.025>

*Total number of authors:*

25

### General rights

Unless other specific re-use rights are stated the following general rights apply:

Copyright and moral rights for the publications made accessible in the public portal are retained by the authors and/or other copyright owners and it is a condition of accessing publications that users recognise and abide by the legal requirements associated with these rights.

- Users may download and print one copy of any publication from the public portal for the purpose of private study or research.
- You may not further distribute the material or use it for any profit-making activity or commercial gain
- You may freely distribute the URL identifying the publication in the public portal

Read more about Creative commons licenses: <https://creativecommons.org/licenses/>

### Take down policy

If you believe that this document breaches copyright please contact us providing details, and we will remove access to the work immediately and investigate your claim.

LUND UNIVERSITY

PO Box 117  
221 00 Lund  
+46 46-222 00 00

Manuscript Number:

Title: Data-flow coupling and data-acquisition triggers for the PreSPEC-AGATA campaign at GSI

Article Type: Full Length Article

Section/Category: Data Acquisition and Control

Keywords: AGATA; PreSPEC; MBS; NARVAL; DAQ; Trigger

Corresponding Author: Mr. Damian Ralet,

Corresponding Author's Institution:

First Author: Damian Ralet

Order of Authors: Damian Ralet; Stéphane Pietri; Yann Aubert; Marco Bellato; Damiano Bortolato; Sergio Brambilla; Franco Camera; Nicolas Dosme; Andres Gadea; Juergen Gerl; Pavel Golubev; Xavier Grave; Håkan T. Johansson; Nabil Karkour; Amel Korichi; Nikolaus Kurz; Xavier Lafay; Eric Legay; Denis Linget; Norbert Pietralla; Dirk Rudolph; Henning Schaffner; Olivier Stezowski; Bruno Travers; Oliver Wieland

Abstract: The PreSPEC setup for high-resolution  $\gamma$ -ray spectroscopy using radioactive ion beams was employed for experimental campaigns in 2012 and 2014. The setup consisted of the state of the art Advanced Gamma Tracking Array (AGATA) and the High Energy  $\gamma$  deteCTOR (HECTOR+) positioned around a secondary target at the final focal plane of the GSI FRagment Separator (FRS) to perform in-beam  $\gamma$ -ray spectroscopy of exotic nuclei. The Lund York Cologne CALorimeter (LYCCA) was used to identify the reaction products. In this paper we report on the trigger scheme used during the campaigns. The data-flow coupling between the Multi-Branch System (MBS) based Data AcQuisition (DAQ) used for FRS-LYCCA and the "Nouvelle Acquisition temps R\`eel Version 1.2 Avec Linux" (NARVAL) based acquisition system used for AGATA are also described.

## Data-flow coupling and data-acquisition triggers for the PreSPEC-AGATA campaign at GSI

D. Ralet<sup>a,b</sup>, S. Pietri<sup>b</sup>, Y. Aubert<sup>c</sup>, M. Bellato<sup>d</sup>, D. Bortolato<sup>d</sup>, S. Brambilla<sup>e</sup>,  
F. Camera<sup>e</sup>, N. Dosme<sup>f</sup>, A. Gadea<sup>g</sup>, J. Gerl<sup>b</sup>, P. Golubev<sup>h</sup>, X. Grave<sup>f</sup>,  
5 H. T. Johansson<sup>i</sup>, N. Karkour<sup>f</sup>, A. Korichi<sup>f</sup>, N. Kurz<sup>b</sup>, X. Lafay<sup>f</sup>, E. Legay<sup>f</sup>,  
D. Linget<sup>f</sup>, N. Pietralla<sup>a,b</sup>, D. Rudolph<sup>h</sup>, H. Schaffner<sup>b</sup>, O. Stezowski<sup>j</sup>,  
B. Travers<sup>f</sup>, O. Wieland<sup>e</sup>, and PreSPEC and AGATA collaboration

<sup>a</sup>*Institut für Kernphysik, Technische Universität Darmstadt, Darmstadt, Germany*

<sup>b</sup>*GSI, Helmholtzzentrum für Schwerionenforschung GmbH, Darmstadt, Germany*

10 <sup>c</sup>*Institut de Physique Nucléaire, Orsay, France*

<sup>d</sup>*Istituto Nazionale di Fisica Nucleare sezione di Padova, Padova, Italy*

<sup>e</sup>*Istituto Nazionale di Fisica Nucleare sezione di Milano, Milano, Italy*

<sup>f</sup>*CSNSM, Université Paris-Sud, Orsay, France*

<sup>g</sup>*Instituto di Fisica Corpuscular, Valencia, Spain*

15 <sup>h</sup>*Department of Physics, Lund University, Lund, Sweden*

<sup>i</sup>*Chalmers University of Technology, Göteborg, Sweden*

<sup>j</sup>*Institut de Physique Nucléaire, Lyon, France*

---

### Abstract

The PreSPEC setup for high-resolution  $\gamma$ -ray spectroscopy using radioactive ion beams was employed for experimental campaigns in 2012 and 2014. The setup consisted of the state of the art Advanced GAMMA Tracking Array (AGATA) and the High Energy  $\gamma$  deteCTOR (HECTOR+) positioned around a secondary target at the final focal plane of the GSI FRagment Separator (FRS) to perform in-beam  $\gamma$ -ray spectroscopy of exotic nuclei. The Lund York Cologne CAlorimeter (LYCCA) was used to identify the reaction products. In this paper we report on the trigger scheme used during the campaigns. The data-flow coupling between the Multi-Branch System (MBS) based Data AcQuisition (DAQ) used for FRS-LYCCA and the “Nouvelle Acquisition temps Réel Version 1.2 Avec Linux” (NARVAL) based acquisition system used for AGATA are also described.

*Keywords:* AGATA, PreSPEC, MBS, NARVAL, DAQ, Trigger

---

*Email address:* [d.ralet@gsi.de](mailto:d.ralet@gsi.de) (D. Ralet)

## 20 1. Introduction

Within the NUclear STructure, Astrophysics and Reactions (NUSTAR) [1] physics program of the Facility for Antiproton and Ion Research (FAIR) [2], physics goal of the HIgh-Resolution In-flight SPECTroscopy (HISPEC) [3] collaboration is to perform high resolution in-beam  $\gamma$ -ray spectroscopy at the final focal plane of the Super-FRS [4] with the AGATA [5] array in conjunction with complementary instrumentation. Similarly, the DEcay SPECTroscopy (DESPEC) [3] collaboration aims to perform stopped-beam experiments employing a wide variety of detectors for comprehensive nuclear decay studies. The two mentioned collaborations will provide detectors built with their own custom-made hardware and Data AcQuisition (DAQ) systems. The PreSPEC collaboration [3] is the precursor of the two above mentioned collaborations, and on top of its own physics program, the task of the PreSPEC collaboration at GSI is also to test the equipment and future technical solutions for HISPEC/DESPEC in view of the challenges associated with FAIR. In this context, the coupling of the conventional in-house “trigger-driven” electronics and DAQ system of the FRS [6], LYCCA [7] and HECTOR+ [8, 9] with the “digital trigger” based electronics and DAQ of the AGATA [5] detector is a proof of concept for NUSTAR at FAIR.

All experiments performed during the PreSPEC-AGATA campaign followed a similar principle [10]. The SIS-18 synchrotron accelerated a primary heavy-ion beam up to 1 GeV/u. The accelerated heavy ions were extracted from the SIS-18 synchrotron in spills of time intervals lasting typically from 1 s to 10 s. The radioactive beams entering the FRS were produced via nuclear reactions on a thick (few g/cm<sup>2</sup>) primary target. The event-by-event-identified radioactive ion-beam particles were impinging on a secondary target placed at the last focal plane (S4) of the FRS. At this point, the produced radioactive ions underwent Coulomb excitation on a gold target or secondary fragmentation on a beryllium target. The  $\gamma$ -ray detectors AGATA and HECTOR+ surrounded the secondary target to obtain nuclear-structure information. Behind the secondary target,

50 the reaction products were identified with LYCCA [7]. The GSI DAQ system  
MBS [11] recorded the data coming from the FRS, LYCCA, and HECTOR+  
detectors, and is described in Sec. 2. The AGATA [5] germanium-detector  
array was read out by fully digital electronics synchronised through the Global  
Trigger and Synchronisation system (GTS) [12]. The AGATA data-flow system  
55 including the GTS and the NARVAL [13] DAQ system is presented in Sec. 3.  
In Sec. 4 the trigger coupling scheme is discussed. A demonstration of the  
performance of the coupled system is given in Sec. 5, prior to a conclusion in  
Sec. 6.

## 2. Description of the PreSPEC DAQ

60 The PreSPEC DAQ system running MBS was responsible for the trigger  
logic and data collection of the full setup except AGATA. Eleven MBS branches  
were used, each consisting of a single VME crate controlled with a RIO3 or  
RIO4 processor [14]. As in a standard MBS system, each crate contained, in  
addition to the controller, a TRIVA trigger module [15]. The TRIVA modules  
65 were linked together via their trigger bus making sure that the system oper-  
ated synchronously on an event-by-event basis. In such a synchronous system,  
the data acquisition runs at the speed of its slowest component. The eleven  
VME crates were positioned between the FRS middle focal point area (S2), the  
FRS end focal point area (S4) and the FRS control room as shown in Fig. 1.  
70 The PreSPEC DAQ was sub-divided into three sub-systems: FRS, LYCCA,  
and GAMMA. Each sub-system consisted of a sub-set of crates and electronics  
modules which are described hereafter.

In each sub-system of the setup Time to Digital Converter with Multi-Hit  
(MH-TDCs) capabilities were used for time measurement. Contrary to a stan-  
75 dard TDC, the MH-TDCs records the time of all hits within a time windows.  
For any event, a few microseconds of the associated memory buffer were written  
to disk. In such case, often several hits per trigger were present. To select the  
“proper hit”, i.e. the one corresponding to the triggering particle, an external  
time reference was fed into four MH-TDC channels. Only one timing signal from

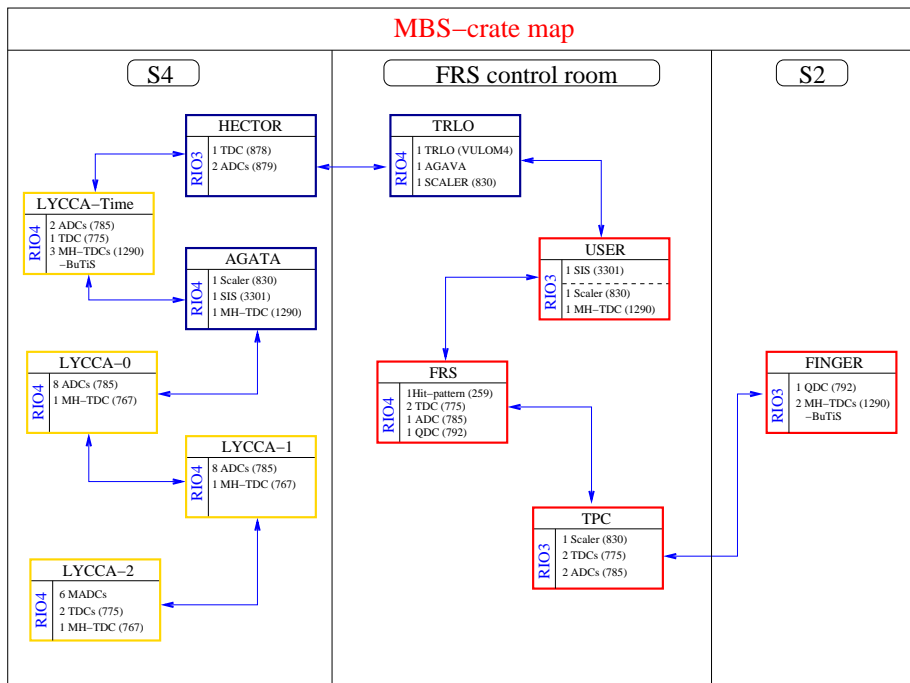


Figure 1: Schematic view of the location of the complex and widely distributed MBS DAQ system of the PreSPEC-AGATA campaign. Each of the eleven VME crates is linked with the trigger bus connection represented by the blue arrow. Each box represents a crate. Red contours denote the FRS sub-system, yellow the LYCCA sub-system and blue the AGATA sub-system. The BuTiS sign means that the MH-TDCs of the crates were synchronised with an external clock. Modules in each crate are listed according to their abbreviations (see text for details).

80 the last focal plane scintillator would have been sufficient, but for redundancy, both left and right scintillator timing signals from the middle and from the final FRS focal plane were chosen.

### 2.1. The FRS sub-system

85 The FRS identification was based on the  $B\rho - \Delta E - B\rho$  method which required the determination of the magnetic rigidity ( $B\rho$ , with  $B$  denoting the magnetic field of a given FRS dipole, and  $\rho$  the bending radius of the magnet [16]) through position determination at the middle and final focal planes and Time of Flight (ToF) measurement of the ion in order to deduce its corresponding  $A/Q$  ratio. Here  $A$  is the mass number of the ion and  $Q$  its charge. An

90 energy loss “ $\Delta E$ ” measurement for the determination of the atomic number  $Z$  of the nucleus [17] was performed at the final focal plane [6]. Four VME crates were dedicated to the read out of the FRS detectors.

The position at each focal plane was determined by Time Proportional Chambers (TPC) [18] all read out by the same crate (cf. Fig 1). Positions  
95 in the dispersive plane of the FRS were determined with TPC delay lines connected to a Time to Digital Converter (TDC, Caen V775). Positions in the vertical plane were given by a measurement of the drift time of the ionized gas with another TDC. In addition, the *TPC crate* hosted two Amplitude to Digit Converters (ADCs, Caen V785) to measure the charge of the TPC electrodes  
100 and a scaler module (Caen V820) for monitoring purposes.

The  $\Delta E$  measurement was done with two Multi-Sampling Ionization Counters (MUSIC) [19] positioned at the S4 final focal plane. The anode signals of the MUSIC detector were amplified and connected to one ADC (Caen V785) of the *FRS crate*. The ToF measurement was performed with conventional plastic  
105 detectors at the middle and final focal plane of the FRS followed by CFDs (Constant Fraction Discriminators) and TACs (Time to Amplitude Converters). Photomultiplier signals of the plastics and TAC signals were sent to the *FRS crate* hosting one Charge to Digital Converter, (QDC, Caen V792) and one ADC. In addition, two TDCs were foreseen for the read out of beam monitoring detectors at other focal points. They were not used during PreSPEC-  
110 AGATA data taking. The *FRS crate* hosted also a hit pattern (Caen V259) module, which received all logic signals from each subsystem to allow either a consistency check with the standard triggering (see below) or, in case of a normalisation trigger, to measure redundantly trigger probabilities.

115 A third crate (called the *USER crate*) was used to assure proper FRS identification in case of high beam intensities. This is relevant for intensities  $\gtrsim 5 \times 10^4$  particles per second at the final focal plane, or in case of an inhomogeneous spill structure. The *USER crate* comprised a ADC-digitizer module (SIS3301) [20] with pile-up disentanglement capabilities for the readout of one of the two MUSICs. In parallel all timing signals (TPCs, scintillators S2/S4, and triggers)  
120

were sent to a Caen V1290 TDC, which has multi-hit capabilities. It was used to perform pile-up determination and served as a backup for the TOF measurement in case the analog chains exhibited problems. The *USER crate* hosted as well one V830 Caen scaler module that monitored counting rates of various  
125 detectors of the experiment as well as the dead time of the full MBS system.

The particle rates at the middle focal plane was much higher than at the last focal plane. For this reason the “finger” detector [21], a plastic detector segmented into 32 strips, was used allowing a ToF measurement at higher rates than the standard middle-focal-plane scintillator. The signals coming from the  
130 photo-multiplier tubes (PMT) of the “finger” detector were split to send one of them to a CFD followed by a MH-TDC for timing purpose, and the other one to a QDC in order to extract charge information related to the strip that fired. Two MH-TDCs (Caen V1290) and one QDC (Caen V792) were hosted inside the *FINGER crate* located in the middle focal plane area. The clock of  
135 the MH-TDCs was synchronised with the one placed at the last focal plane area using the BuTiS [22].

## 2.2. The LYCCA sub-system

The particle identification in LYCCA was based on a  $E$ -ToF (mass  $A$ ) and  $E - \Delta E$  (charge  $Z$ ) measurement [7]. In addition, LYCCA provided tracking  
140 of the reaction products after the secondary target. Circular membrane plastic scintillators [23] with multiple PMT readout, were used as start and stop for the ToF measurement. Two start plastic detectors were available, one with 32 PMTs (diameter 27 cm) located  $\sim 1.0$  m in front of the secondary target, and a second one, the target ToF, with 12 PMTs (diameter 7.3 cm) at about 10 cm before the  
145 secondary target. The stop plastic had 32 PMTs and was located  $\sim 3.0$  m behind the secondary target. The time signals from the PMTs were read out with 3 MH-TDCs (Caen V1290) located in the *LYCCA-time crate*. The clock of the MH-TDCs were synchronised with the one of the *FINGER crate* via BuTiS [22]. In addition, the *LYCCA-time crate* hosted two ADCs (Caen V785) to record  
150 the energy signals of all 32x32 strips of the target Double Sided Silicon Strip



Detector (DSSSD) which provided the interaction position on the target [7]. An extra TDC in common stop (Caen V775) was located in this crate for the target DSSSD timing signals used for hit distinction during experiments with high S4 rate.

155 The  $E - \Delta E$  measurement was obtained from the LYCCA wall that consisted of 16 telescopes. Their front part made of 32x32 strips DSSSD detectors for  $\Delta E$  and position measurement were attached to a stack of nine CsI crystals (CsI) for the total energy measurement [7]. The strips of the DSSSD wall modules were connected in pairs and fed into STM-16+ Mesytec shapers [24]. 16 ADCs (Caen  
160 V785) and two MH-TDC (Caen V767) in both the *LYCCA-0 crate* and *LYCCA-1 crate* received the energy and the time outputs of the shapers, respectively.

The CsI signals went into MSCF-16 shapers and further to six Mesytec ADC (MADC-32). Their timing signals were processed by one MH-TDC (Caen V767) and two TDCs (Caen V775). These nine modules were hosted in the *LYCCA-2*  
165 *crate*.

### 2.3. The GAMMA sub-system

The HECTOR+ detector array was composed of ten large volume LaBr<sub>3</sub>:Ce scintillators and eight large volume BaF<sub>2</sub> scintillators. The readout and acquisition of HECTOR+ signals was done with the *HECTOR crate*. In this crate, two  
170 ADCs (Caen V879) and one TDC (Caen V878) were present. They recorded two dynamic ranges for the LaBr<sub>3</sub>:Ce scintillators in order to cover low and high energy  $\gamma$ -rays, and their time. In addition, two time components (slow and fast) of the BaF<sub>2</sub> detectors were recorded in order to allow neutron- $\gamma$  discrimination and to fully use their good intrinsic time resolution. The energy read-out of the  
175 BaF<sub>2</sub> scintillators had only one range.

The *AGATA crate* consisted of one MH-TDC (Caen V1290) and one scaler module (Caen V830) in which each Germanium core signal was sent after passing through a Timing Filter Amplifier (TFA) and CFD. In addition, the crate hosted a flash-ADC module (SIS-3301) in which seven core energy signals were read  
180 out. This crate was set mainly for monitoring of the  $\gamma$ -part of the trigger (Sec. 4)

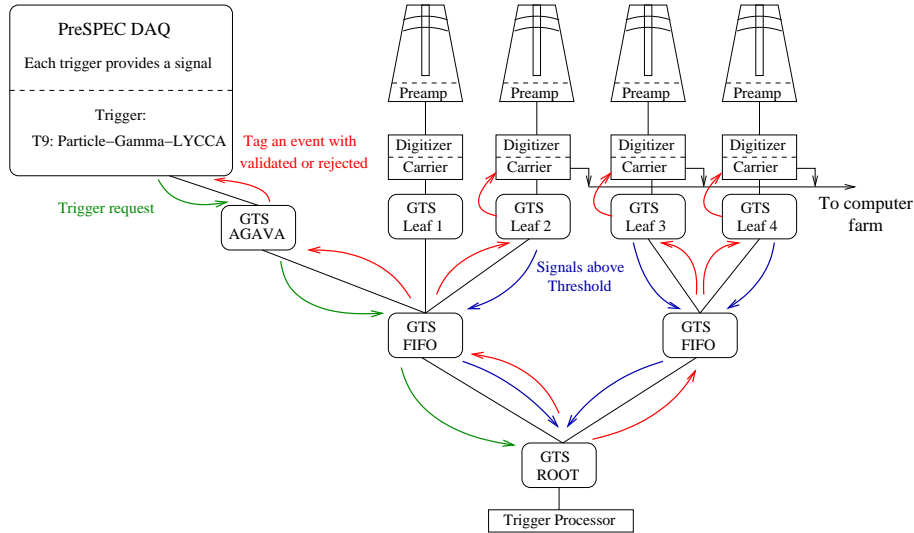


Figure 2: The core output of each crystal was connected to a GTS configured as leaf of the GTS tree (see text for details). Every time a core had a signal above threshold, a request was sent to the root of the tree connected to the trigger processor (blue arrows). One other leaf (GTS AGAVA) represented the complementary detectors of the PreSPEC setup. It sent a request to the trigger processor for each validated MBS trigger (green arrows). The trigger processor performed the coincidence, and validated  $\gamma$ -ray events in coincidence with PreSPEC ancillary detectors (red arrows). Validated events were read by the computer farm.

and for consistency checks of the data coupling (see Sec. 5).

The master crate in the setup was called *TRLO crate*. It assured the synchronous read out of all the crates for a given Master trigger. Master triggers were generated by the TRigger LOGic (TRLO) firmware [25–27] (Sec. 4) installed  
 185 on a VULOM4 [28] that handled dead-time locking and read-out decisions taken according to the user-defined scheme (Sec. 5).

In addition, the *TRLO crate* included an AGAta VME Adaptateur (AGAVA) [5] that provided the possibility to couple VME-based system to the AGATA system and the GTS time-stamp information for any MBS event (Sec. 3).

### 190 3. The AGATA data flow at GSI

#### 3.1. Pre-processing stage of the AGATA data flow

The 36 segments and two core signals (two gains for each core were available during the GSI experiments: 5 MeV and 30 MeV full range) coming from the

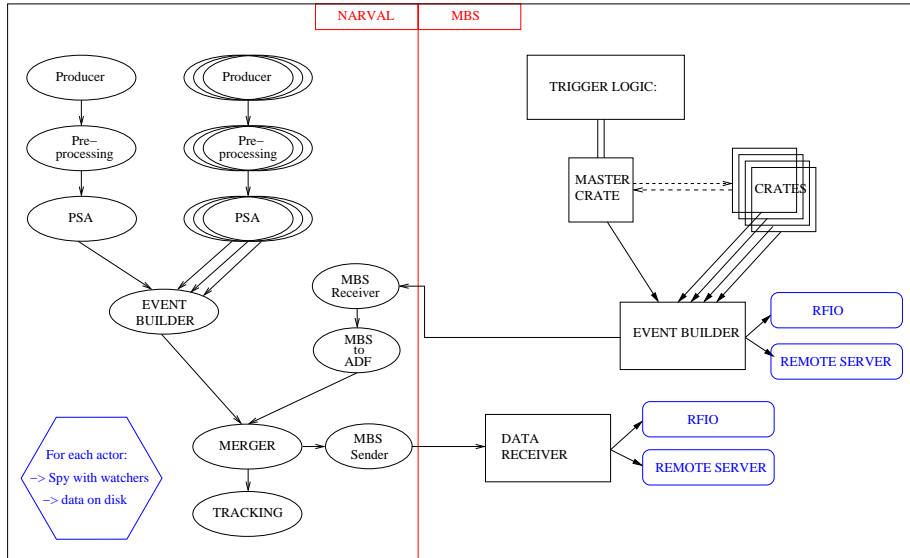


Figure 3: Scheme of the data flow coupling for the AGATA and MBS DAQ system. On the left hand side are shown the different actors of NARVAL that were needed to process the data flow. The right hand side depicts the MBS DAQ systems, with the different crates reading out the data of the PreSPEC ancillary detectors, together with the MBS data flow (see text in Sec. 2 for details).

pre-amplifiers of each segmented HPGe detectors were sampled by 100 MHz,  
 195 14-bit flash-ADCs of the digitizers. They were running with a common clock  
 received by the GTS. The 38 digitized signals were sent via optical fibers to  
 the pre-processing stage. The latter was composed of mezzanine cards hosted  
 on ATCA carriers boards [5]. Mezzanines processed the data, i.e. extracted  
 the energy information via a digital trapezoidal filter, or a Moving Window  
 200 Deconvolution (MWD) algorithm [29]. Timing information was extracted using  
 a leading-edge algorithm. For any core signal above noise level, time, energy,  
 and trace (100 samples) of the core and segment digital signals (pulse shape)  
 were stored inside the mezzanine memory. The GTS system assured the time-  
 stamping of this data on a 48-bit stamp with a step of 10 ns. The mezzanines  
 205 stored the data until a decision from the trigger processor (see next paragraph)  
 was received to either validate or discard the events. In the case of event vali-  
 dation, all the mezzanines sent their data to their carrier. The latter built and

pushed the event to the computer farm.

### 3.2. The Global Trigger and Synchronisation System

210 The AGATA triggering system, called GTS, was built as a tree, where each germanium detector corresponds to a leaf. In the tree philosophy, each leaf was sending a trigger request to the trigger processor unit connected to the root of the tree (see illustration in Fig. 2).

In the preprocessing electronics, the threshold was set slightly above noise  
215 level to allow a good base-line determination in the MWD process, assuring the best possible energy resolution. Each crystal that had its core signal crossing this threshold provided a trigger request to the GTS tree that forwarded the request to the root GTS connected to the trigger processor [12]. The latter either validated or rejected the trigger request. It sent the decision via the tree to the  
220 requesting GTS, and the associated event was either read by the computer farm or discarded. A reduced scheme of the GTS tree configuration as used for the experiments is shown in Fig. 2. The GTS decision to validate or reject depended on the trigger processor configuration. In the “standard” PreSPEC configuration two partitions were set: one containing all the Germanium detectors, and  
225 the other one containing the trigger request from the particle detector, or ancillary detector. Each partition that had at least one request set the partition “up” for  $1 \mu\text{s}$ . A coincidence between the two partitions was set if both of them were “up” for  $6 \mu\text{s}$  with the coincidence window set to  $-/+ 3 \mu\text{s}$  around the ancillary request. Each GTS-leaf (detectors or ancillary leaf) that had a request in the  
230 coincidence window was validated. With this trigger processor configuration, the full system got validated by the VME-based electronics. This solution was chosen in order to be able to couple an analog system with a fully digital one. The trigger decision inside the GTS system was taking at least  $10 \mu\text{s}$  and it was not possible to wait that long in the PreSPEC analog branch before processing  
235 the event. Consequently the read-out of the coupled system was controlled by the trigger decision from the TRLO firmware. This solution was devised also to allow to have a different threshold for the particle- $\gamma$  coincidence regardless of

any effect on the MWD filter applied in the pre-processing stage. We operated usually with higher  $\gamma$ -ray thresholds for the coincidence, cutting most of the  
240 Lorentz boosted X-rays generated by the slowing down process of the incoming beam in the detectors and target material. This feature proved to be invaluable for heavy  $Z$  beam on high  $Z$  target, where the particle- $\gamma$  trigger would have otherwise been drowned in background.

The GTS system had also the possibility to be used in an “isomer tagging”  
245 configuration in order to measure the decay of an isomeric state from an ion stopped by a catcher in front of the AGATA detectors. In that case, the ancillary partition was set with a window of  $1 \mu\text{s}$ , the germanium partition with a window of  $10 \mu\text{s}$  and the coincidence window was set to  $-11/+2 \mu\text{s}$ . If a prompt photon is emitted with the beam implantation, the system was recording all consecutive  
250  $\gamma$ -ray decays during the next  $10 \mu\text{s}$  of the “up”  $\gamma$  partition. With no prompt  $\gamma$ -ray, the system would record an isomer decaying in the following  $11 \mu\text{s}$  after implantation due to the coincidence window. By consequence, this configuration allowed the measurement of isomers, with a lifetime between a few hundred nanoseconds and several microseconds. The implantation rate had to be limited  
255 to a few kilohertz in order to avoid the  $\gamma$  partition to be set “up” continuously, i.e. until the next implanted ion, and because the minimum bias trigger was used as main trigger to operate the MBS DAQ with limited dead-time.

### 3.3. Data flow handling with NARVAL

Each event, as validated by the GTS, comprised energy, time-stamp and  
260 traces from the 36 segments and the core of each germanium crystal. This information was processed in computer farms with the so-called “actors” of NARVAL [30]. As shown on the left side of the scheme in Fig. 3, the topology (or set of actors) for each crystal consisted of three main elements. The first actor, *Producer*, collected the data from the carriers. The second actor, *Pre-*  
265 *Processing*, performed the time and energy calibration of the core and each segment with a hit. Then a third actor, the Pulse Shape Analysis *PSA*, extracted from the pulse shapes the interaction positions of each detected  $\gamma$  ray using a

grid-search algorithm [31]. Afterwards, an actor *Event-Builder* built the event according to related time-stamps, i.e., constructed an event with data coming from different crystals. A second building stage, the *Merger*, allowed the merging of the PreSPEC detector data with the AGATA data flow as explained in Sec. 5. The positions and energies of each interaction point of all  $\gamma$  rays were used by the *Tracking actor* [32] in order to reconstruct the full energy of a Compton scattered  $\gamma$  ray from all associated interaction points.

Each actor had the possibility to write data encoded with the AGATA Data Format (ADF) [33] on disk. During all the GSI experiments, data were written at the level of the actor *Producer* in order to allow a “replay” of the data if post-experiment calibrations were needed. The data after the PSA algorithm were written for on-line and off-line analysis after *Event Builder*, *Event Merging* and *Tracking*. In addition, the data flow was monitored by Watchers [33] that spied each NARVAL actor.

#### 4. Triggering the system

The processing time of a PreSPEC-AGATA event by the MBS was at least 90  $\mu$ s. The DAQ system was operated with particle rates at the final focal plane of up to  $10^5$  particles per second. It was therefore not possible to record an event for every particle hitting the last FRS plastic detector (SC41). In addition, even though the AGATA system could operate in an almost trigger-less mode, the corresponding amount of raw data (mainly AGATA traces) would have been up to  $\sim 40$  TB per day. A trigger selection was mandatory to avoid the costs of preparing a storage infrastructure able to deal with this amount of data.

The complexity of the setup implied a complex trigger scheme, capable of optimizing the data storage and to handle the coupling of both sub-systems.

##### 4.1. Generation of the trigger request signals

Online  $\gamma$ -ray spectroscopy with the PreSPEC setup required to record  $\gamma$ -ray events in coincidence with an identified heavy ion in both FRS and LYCCA. The fast plastic scintillator (SC41) placed before the secondary target provided

the particle trigger request. In order to have a  $\gamma$ -trigger request, copies of the AGATA detector core preamplifier signals were sent to Timing Filter Amplifiers (TFAs), gain matched, and cabled to two remotely controlled CFDs. A logic *OR* of all the signals from these CFDs was sent to the trigger logic module. The HECTOR trigger request was an *OR* of all the detector crystals with a preceding coincidence performed with the SC41 plastic scintillator. This solution was chosen to start the event processing as soon as possible by the *HECTOR crate* electronic modules. This was done in order to avoid a delay of a few hundred nanoseconds due to cable length between the FRS final focal plane area and the FRS control room and allowed to maintain a good energy resolution for the HECTOR+ detectors. Data were then validated and readout only when the master trigger arrived. The HECTOR VME modules were otherwise cleared.

Due to geometrical efficiency limitation, typically 50% of the events hitting the SC41 detector did not reach the LYCCA DSSSD wall and an event without LYCCA information cannot be Doppler corrected. In order to increase the number of proper events recorded on disk that had a hit in the LYCCA wall, a coincidence with LYCCA signals was included in the trigger. A systematic analysis of different trigger combinations for LYCCA was performed during the technical commissioning of the PreSPEC-AGATA system. Following this analysis, the LYCCA trigger request (LYCCA-OR) was defined as a hit in the target ToF plastic scintillator together with a hit in the DSSSD Wall. This provided the minimum information needed for ion tracking and identification in LYCCA.

#### 4.2. Description of the trigger logic

The trigger scheme consisted of twelve different triggers firing only when the acquisition was not busy processing an event. Each trigger was associated with a particular event configuration. Trigger 12, *spill-on* trigger, fired at the beginning of the beam extraction from the SIS-18 synchrotron. Trigger 13, *spill-off* trigger, fired at the end of the beam extraction. Trigger 10 was a particle trigger generated for each SC41 trigger request. This trigger corresponded to

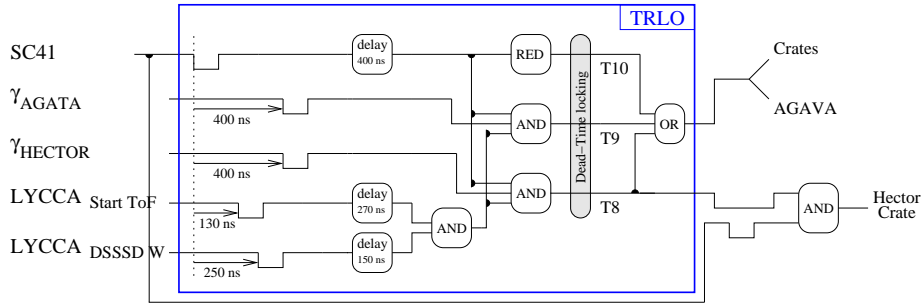


Figure 4: The drawing shows the generation of three physics' trigger: 8, 9, and 10. The blue box highlights the logic performed inside the FPGA of the VULOM4 with the TRLO firmware.

a trigger that read-out the full system independently of the physics process that occurred at the secondary target. In addition, it depended only on the particle detection efficiency of a single detector. Therefore, it was the minimum bias trigger. It was used with a selectable reduction factor as a normalisation trigger. Trigger 10 was also used without reduction during isomer measurements (isomer tagging configuration). Physics triggers (6-9) required a coincidence with a particle (SC41 signal), a LYCCA signal and with a  $\gamma$ -ray detected in AGATA (trigger 9) or in HECTOR (trigger 8). Trigger 7 and 6 were the same as trigger 9 and 8 respectively, without the coincidence with the LYCCA signal. Trigger 5 was a generic FRS trigger. It was used during the set up of the FRS, and could be switched to any FRS detector. Triggers from 2 to 4 were calibration triggers used for the calibration of HECTOR (trigger 4), AGATA (trigger 3), and LYCCA (trigger 2). Trigger 1 was a scaler readout trigger. It ran at 10 Hz, and was always validated (it stayed pending until the dead time was released).

Triggers with higher number took priority, e.g. trigger 10 had a higher priority than trigger 9.

This trigger scheme was implemented on a Field Programmable Gate Array (FPGA) in a module developed at GSI, the VULOM4 [28], with the help of the TRLO firmware. Trigger request signals were stretched to 150 ns, time



aligned and sent to a logic unit that continuously evaluated the coincidences. A trigger was generated if all associated signals were present at one clock cycle. The TRLO logic waited for 100 ns and during that time assigned the trigger number according to the coincidence scheme. The trigger was accepted if the PreSPEC DAQ system was not processing another event. The timing of the different trigger requests for a part of the configuration can be seen in Fig 4.

Gates were generated and were sent to the different modules of the crates according to the trigger number as shown in Table 1. In addition, all triggers latched all scaler modules in any of the eleven VME crates.

Table 1: Gate generation for the different triggers. The gates were sent to all the modules of FRS, HECTOR, AGATA, and LYCCA crates.

Trigger	FRS	AGAVA	HECTOR	AGATA	LYCCA	Scalers
1		X				X
2		X			X	X
3	X	X		X		X
4		X	X			X
5	X	X			X	X
6, 7, 8, 9, 10	X	X	X	X	X	X
12, 13	X	X				X

For any accepted trigger, a gate to the AGAVA (as shown in Table 1) was sent. This gate triggered the GTS system setting the ancillary partition to “up” (Sec. 3). Inside any MBS event a tag (validated or rejected) from the AGAVA, i.e. the GTS system, was written in addition to the GTS time-stamp. For both GTS tags, MBS data were written on disk. It assured the data to be recorded for a trigger 8, where a clear of the MBS event in case of a GTS rejection flag would have discarded an event with a  $\gamma$  ray detected by HECTOR.

## 5. Coupling of the DAQ systems

### 5.1. Principle

As mentioned above, the MBS system was based on several branches, connected to each other via a trigger bus, which assured the synchronisation of the data. For each TRIVA validated trigger, the data words of each crate were read

out by the VME crate backplanes (sub-event), and were sent via network to an event builder. The data were written on disk at the level of the event builder. A  
370 schematic view of the MBS data flow structure can be found on the right hand side of the scheme in Fig. 3.

The “built” data from MBS was sent to the AGATA computer farm via an Ethernet connection received by a specific NARVAL actor called *MBS Receiver*. The actor *MBS to ADF* encapsulated the MBS data in an ADF format. Each  
375 MBS event had a GTS time-stamp (Sec. 4) and was written on disk in the ADF format to allow off-line data merging (in case of re-calibration needs for AGATA). The MBS data were merged with the AGATA “built” data by the actor *Merger* using the GTS time-stamps. In Fig. 3 the scheme of the full data flow including the MBS event building, the AGATA data processing, and the  
380 coupling of MBS and AGATA data flow is illustrated.

The last NARVAL actor (Fig. 3), the actor *MBS Sender*, and its associated MBS receiver were sending back all information in the MBS data format. This enabled a simpler online analysis.

### 5.2. System integrity check

385 The first verification was performed by an MBS process, the *Time Sorter*, that performed a one to one data analysis. It checked that any event sent to NARVAL was built and properly sent back to the MBS receiver. No missing events were seen.

As explained before, any MBS event got a tag from the GTS system through  
390 the AGAVA in order to indicate if the event was accepted or rejected by the GTS. The tagging information showed that in case of a trigger 9, i.e. *Particle- $\gamma_{AGATA-LYCCA}$* , more than 99.9% of the events were accepted by the GTS system.

In order to be able to verify the proper synchronisation between MBS and  
395 the AGATA data flow, seven AGATA core signals were digitized within the MBS DAQ (see Sec. 2). The two-dimensional histogram in Fig. 5 proves the correlation between data coming from AGATA itself (*y*-axis) and the one generated

within MBS ( $x$ -axis). The diagonal line shows proper correlation of the data after data-merging. The MWD algorithms used with the SIS module and AGATA  
 400 electronic had different parameters which can explain most of the events with different energies seen outside the diagonal.

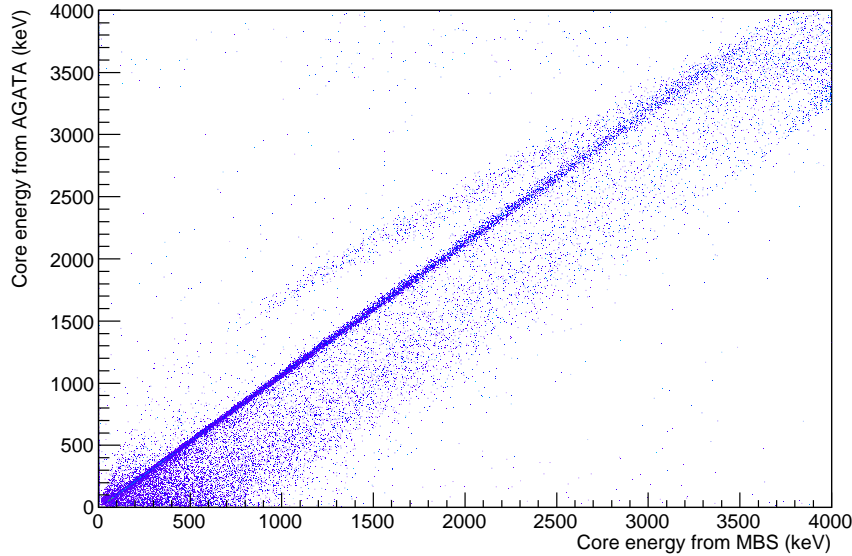


Figure 5: Core energy of one crystal in the MBS data acquisition digitized by the SIS module as a function of the core energy obtained with the AGATA electronics and computer farm.

A good behaviour of the system was seen as well with the isomer setting (see Sec. 3), when both data from PreSPEC ancillary detectors and from AGATA had to be present and correlated. The time information is also needed to see the  
 405  $\gamma$ -ray decay occurring from 100 ns to a few  $\mu$ s after the implantation. A time versus energy  $\gamma$ -ray spectrum is shown in Fig. 6, with the observation of the decay of the  $^{109}\text{Rh}$  isomeric state that has a half life of  $T_{1/2} = 1.66(4) \mu\text{s}$  [34].

A last validation test for the system correlation was performed using in flight emitted X-rays, which have a large production cross-section. The data  
 410 correlation is essential in order to be able to see the angular dependence of the X-rays after Doppler correction as shown in Fig 7. The two  $K_{\alpha}$  X-rays of

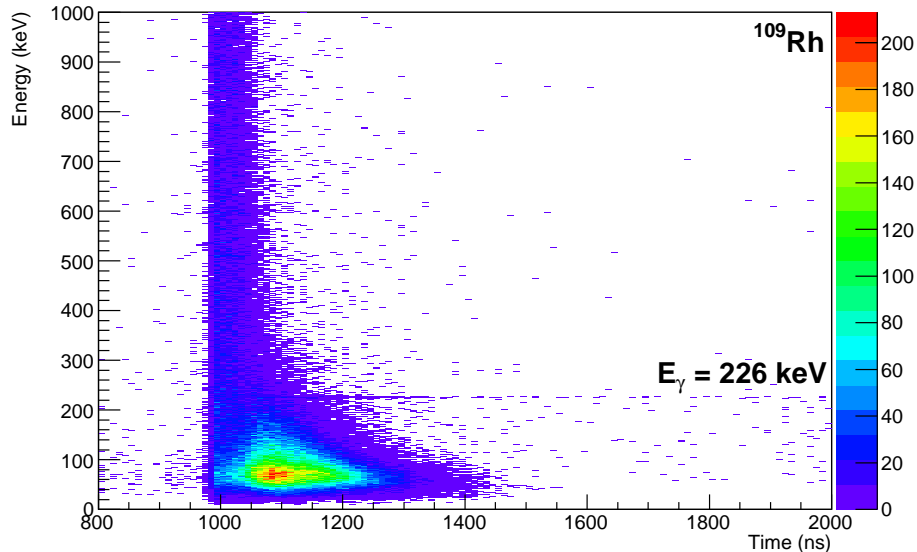


Figure 6: Time versus energy spectrum for an isomeric state in  $^{109}\text{Rh}$ . The transition at  $E_\gamma = 226$  keV belongs to the decay of a  $T_{1/2} = 1.66(4)$   $\mu\text{s}$  isomeric state [34].

Uranium at 94.6 keV and 98.4 keV were clearly identified and proved that both MBS and AGATA data sets were correlated.

## 6. Conclusion

415 The coupling of the data flow, triggered by the analog MBS system and the digital GTS, showed good results and provided a proof of principle of the flexibility of MBS and AGATA. Indeed, the data taken by both AGATA and MBS were consistent, and proper analysis on an event-by-event basis is possible. The data integrity was confirmed with test cases such as isomers and particle-X-  
 420 ray correlations. An additional integrity test was performed using an MBS *Time Sorter* where any MBS event was correlated to the same event after passing the NARVAL system.

The coupled DAQ at GSI was used for eight experiments in 2012 and 2014, and produced almost 200 TB of data including calibrations. The system was

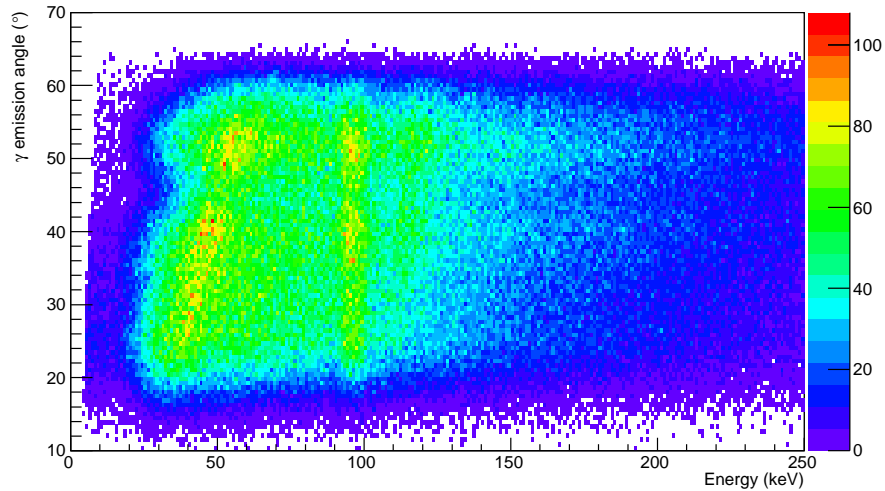


Figure 7: Angle of the  $\gamma$ -ray emission in AGATA as a function of the Doppler-corrected  $\gamma$ -ray energy. The straight vertical line slightly below 100 keV corresponds to a superposition of the two  $K_{\alpha}$  X-rays of  $^{238}\text{U}$  ions after Doppler correction using the outgoing velocity and tracking information from LYCCA. This proved the correlation between AGATA and MBS data.

425 pushed up to 3 kHz of event data for MBS, and around 3 kHz of validated events per AGATA crystal. Up to 22 working AGATA crystals were in the setup.

The limiting factor of the system was its dead time. The total number of events recorded on disk per second was in standard utilisation limited to few kilohertz. The dead time mainly originated from the RIO3 VME controller used for the TPC crate. Therefore a RIO4 exchange has been foreseen for future  
 430 experiments. In addition, the spill structure due to the slow extraction from the SIS-18 synchrotron was affecting the total throughput. Diagnostic tools in the TRLO firmware were readily used to help beam operators optimize beam settings.

435 A possible improvement could be performed on the particle- $\gamma$  coincidence. A huge contribution of the recorded events came from high energy events: charged particles passing through the AGATA detectors. An anti-coincidence on an upper  $\gamma$ -ray threshold could be applied to improve the ratio of interesting events over background. Adding an energy loss condition from the MUSIC detectors

440 inside the trigger can help to remove contributions from charged particles lighter  
than the ones of interest thus also improve the maximal throughput of the  
system.

## 7. Acknowledgments

This work was supported by the BMBF under Nos. 05P09RDFN4, 05P12RDFN8,  
445 and by the LOEWE center HIC for FAIR.

This work has also been supported by the European Community FP7 -  
Capacities, contract ENSAR n 262010, and by the Swedish Research council.

One of the authors, A. Gadea, was partially supported by MINECO, Spain,  
under the Grant FPA2011-29854-C04 and Generalitat Valenciana, Spain, under  
450 the Grant PROMETEOII/2014/019.

## References

- [1] NUSTAR. URL: [http://www.fair-center.eu/for-users/  
experiments/nustar.html](http://www.fair-center.eu/for-users/experiments/nustar.html).
- [2] FAIR, Baseline Technical Report. URL: [http://www.fair-center.eu/  
455 for-users/publications/fair-publications.html](http://www.fair-center.eu/for-users/publications/fair-publications.html).
- [3] Z. Podolyak, Nuclear Instruments and Methods in Physics Research Section  
B: Beam Interactions with Materials and Atoms 266 (2008) 4589 – 4594.  
Proceedings of the {XVth} International Conference on Electromagnetic  
Isotope Separators and Techniques Related to their Applications.
- 460 [4] M. Winkler, et al., Nuclear Instruments and Methods in Physics Research  
Section B: Beam Interactions with Materials and Atoms 266 (2008) 4183 –  
4187. Proceedings of the {XVth} International Conference on Electromag-  
netic Isotope Separators and Techniques Related to their Applications.
- [5] S. Akkoyun, et al., Nuclear Instruments and Methods in Physics Research  
465 Section A: Accelerators, Spectrometers, Detectors and Associated Equip-  
ment 668 (2012) 26 – 58.

- [6] H. Geissel, et al., Nuclear Instruments and Methods in Physics Research Section B: Beam Interactions with Materials and Atoms 70 (1992) 286–297.
- [7] P. Golubev, et al., Nuclear Instruments and Methods in Physics Research  
470 Section A: Accelerators, Spectrometers, Detectors and Associated Equip-  
ment 723 (2013) 55 – 66.
- [8] A. Giaz, et al., Nuclear Instruments and Methods in Physics Research Sec-  
tion A: Accelerators, Spectrometers, Detectors and Associated Equipment  
729 (2013) 910 – 921.
- 475 [9] F. Camera, et al., EPJ Web of Conferences 66 (2014) 11008.
- [10] N. Pietralla, et al., EPJ Web of Conferences 66 (2014) 02083.
- [11] H. Essel, et al., Nuclear Science, IEEE Transactions on 43 (1996) 132–135.
- [12] M. Bellato, et al., Nuclear Science, IEEE Transactions on 55 (2008) 91–98.
- [13] X. Grave, et al., in: Real Time Conference, 2005. 14th IEEE-NPSS, 2005,  
480 p. 5.
- [14] CES, VME Single Board Computers. URL: [http://www.ces.ch/  
board-products/vme-single-board-computers](http://www.ces.ch/board-products/vme-single-board-computers).
- [15] J.Hoffmann, et al., TRIVA, VME Trigger Module, GSI, 2003.
- [16] H. Wiedemann, Particle Accelerators Physics, Springer 3rd Edition, 2007.
- 485 [17] W. R. Leo, Techniques for nuclear and particle physics experiments: a  
how-to approach, Springer, 1994.
- [18] V. Hlinka, et al., Nuclear Instruments and Methods in Physics Research  
Section A: Accelerators, Spectrometers, Detectors and Associated Equip-  
ment 419 (1998) 503 – 510.
- 490 [19] A. Stolz, et al., Phys. Rev. C 65 (2002) 064603.

- [20] Struck-Innovative-System, SIS3301 8 CHANNEL 105 MS/S 14-BIT ADC/DIGITIZER. URL: <http://www.struck.de/sis3301.htm>.
- [21] F. Ameil, et al., GSI scientific report 2010 GSI Report-1 NUSTAR-FRS (2011) 171.
- 495 [22] D. Beck, Timing System Butis Interface. URL: <https://www-acc.gsi.de/wiki/Timing/TimingSystemButisInterface>.
- [23] R. Hoischen, et al., Nuclear Instruments and Methods in Physics Research Section A: Accelerators, Spectrometers, Detectors and Associated Equipment 654 (2011) 354 – 360.
- 500 [24] Mesytec, Overview of Mesytec modules. URL: <http://www.mesytec.com/silicon.htm>.
- [25] H. T. Johansson, et al., GSI scientific report 2010 GSI Report-1 IS-EE (2011) 231.
- [26] D. Ralet, et al., GSI scientific report 2011 GSI Report-1 NUSTAR-FRS  
505 (2012) 170.
- [27] D. Ralet, et al., GSI scientific report 2012 GSI Report-1 ENNA-EXP (2013) 180.
- [28] VULOM, Vulom Manual. URL: [http://www.gsi.de/informationen/wti/ee/fertigung/module\\_datenpflege\\_e.html](http://www.gsi.de/informationen/wti/ee/fertigung/module_datenpflege_e.html).
- 510 [29] A. Georgiev, et al., Nuclear Science, IEEE Transactions on 41 (1994) 1116–1124.
- [30] N. Lalović, Eur. Phys. J. Web of Conferences, in press (2015).
- [31] R. Venturelli, et al., LNL Annual Report (2004).
- [32] A. Lopez-Martens, et al., Nuclear Instruments and Methods in Physics  
515 Research Section A: Accelerators, Spectrometers, Detectors and Associated Equipment 533 (2004) 454 – 466.



- [33] O. Stezowski, GammaWare Head Version for release 0.9. URL: <http://www.ipnl.in2p3.fr/gammaware/doc/html/>.
- [34] N. Kaffrell, et al., Nuclear Physics A 470 (1987) 141 – 160.